

Photophysical properties of 2,3,6,7-tetrahydro-8-hydroxy-1H, 5H-benz[*i,j*] quinolizine-9-carboxaldehyde: Evidence of excited state intramolecular proton transfer but not of intramolecular charge transfer process

Subrata Mahanta^a, Rupashree Balia Singh^a, Debnarayan Nath^b, Nikhil Guchhait^{a,*}

^a Department of Chemistry, University of Calcutta, 92 A. P. C. Road, Kolkata 700009, India

^b Department of Physical Chemistry, Indian Association for the Cultivation of Science, Jadavpur, Kolkata 700032, India

Received 7 September 2007; received in revised form 26 November 2007; accepted 12 December 2007

Available online 23 December 2007

Abstract

The photophysical behaviours of 2,3,6,7-tetrahydro-8-hydroxy-1H, 5H-benzo[*i,j*] quinolizine-9-carboxaldehyde (THBQC), a molecule having both the intramolecular excited state donor acceptor charge transfer and six member intramolecular hydrogen bonded proton transfer sites, have been investigated by steady state and time resolved spectroscopy in combination with quantum chemical calculations. The observed spectral characteristics of THBQC with variation of solvent properties, pH and temperature of the medium confirm the existence of different neutral and ionic species in the ground and excited states. Comparatively less solvent polarity dependent red shifted emission band of THBQC in all solvents is attributed to excited state intramolecular proton transfer of the closed conformer leading to keto-enol tautomerism but not of intramolecular charge transfer process. In polar solvents, apart from the proton transfer emission band, another band at higher energy region is attributed to the emission from the open solvated form. Evaluation of the potential energy surfaces by quantum chemical calculations using Density functional theory (DFT) and Hartree–Fock (HF) levels point towards the possibility of proton transfer reaction in the first excited state and correlate well with the experimental findings.

© 2007 Elsevier B.V. All rights reserved.

Keywords: 2,3,6,7-Tetrahydro-8-hydroxy-1H, 5H-benzo[*i,j*] quinolizine-9-carboxaldehyde (THBQC); Excited state proton transfer (ESIPT); Keto-enol tautomerism; Fluorescence; Density functional theory

1. Introduction

Proton and charge transfer are the two most fundamental processes involved in different chemical reactions and in the living systems [1–9]. Photoinduced proton transfer and charge transfer reactions have attracted the attention of many research groups from fundamental and application point of views. The excited state intramolecular proton transfer (ESIPT) process and the dual fluorescence of methyl salicylate were first reported by Weller in 1956 [1]. After this pioneering report, many studies have been devoted to a variety of molecular systems to explore the detailed understanding of proton transfer process both experimentally and theoretically. It is found that an intramolecular hydrogen bond (IMHB) between the proton donor and accep-

tor moieties in the ground state facilitates proton transfer upon photoexcitation [10–13]. Such an excited state proton transfer process shows characteristic low energy emission and this emission is less solvent polarity sensitive. Simultaneously, studies of excited state intramolecular charge transfer (ICT) reaction also attracted the attention of various research groups after the first observation of dual fluorescence from the benchmark molecule dimethylaminobenzonitrile (DMABN) [3]. The typical examples of these ICT systems have a variety of donor and acceptor groups tagged to a variety of chromophores [4]. In this type of ICT process, charge transfer occurs in the excited state and a characteristic solvent polarity dependent emission is observed from the highly polar charge transfer (CT) state. For years, the literature on ESIPT and ICT has become richer and richer not only due to fundamental interest but also due to their vast applications in the form of laser dyes and LED [14–15], UV photo stabilizers [16–17] and fluorescent sensors [18–19] and molecular switches [20–22].

* Corresponding author.

E-mail address: nguchhait@yahoo.com (N. Guchhait).

Apart from experimental study, the exploration of the potential energy surfaces in the ground and excited states have also become a field of active research [23–27]. In case of proton transfer process in orthohydroxy benzaldehyde (OHBA), the normal species with an IMHB is the stable conformer on the ground state potential energy surface whereas on the excited state potential energy surface, the keto conformer is the stable one [28–34]. The spectral features of such systems are the exothermal behaviour of the excited singlet state potential curve and endothermal behaviour in the ground state potential energy curve. It is now well established that proton transfer (PT) itself can proceed on the subpicosecond time scale [35–38]. The ESIPT process proceeds adiabatically on the S_1 hyper-surface [23,27] whereas the internal conversion (IC) channel is due to a surface crossing or a conical intersection and occurs on varying time scales [37,39–41]. In case of ICT process quite a few number of models such as twisted intramolecular charge transfer (TICT), [3,4] planar intramolecular charge transfer, [42] wagging intramolecular charge transfer [43] and rehybridized intramolecular charge transfer [44] have been proposed so far. According to the most accepted TICT model by Grabowski et al. the excited state PES shows a second minima along the twisting motion of the donor group which leads to a solvent polarity dependent red shifted emission from the CT state [3,4].

Molecules of diverse complexities have been studied but the most important and interesting ones are those with bifunctional groups having both the proton donor–acceptor and the charge donor–acceptor abilities within the same system. In most cases, the PT and the ICT can be considered to be decoupled, as observed in the ultrafast pump-probe experiments [45]. Such types of systems tend to exhibit stronger acidity and basicity in the excited state leading to transfer of proton from acidic to basic moiety and also have the ability of charge transfer from donor to the acceptor group upon excitation. This leads to a normal fluorescence from the locally excited state together with a Stokes-shifted emission from the keto tautomer or the excited CT state. However, the most vivid distinction between the red shifted emission from ESIPT and CT state is that the position of the CT emission band shows large solvent polarity dependence compared to that of ESIPT emission band. In this study, photophysical properties of 2,3,6,7-tetrahydro-8-hydroxy-1H, 5H-benzo[*i,j*] quinolizine-9-carboxaldehyde (THBQC) have been investigated spectroscopically. The molecule THBQC is a unique compound having both the prerequisite intramolecular ESIPT and ICT sites. So far our knowledge goes there has been no photophysical study for this molecule. The excited state proton translocation site in THBQC is similar to that of the studied system orthohydroxybenzaldehyde (OHBA) [2,28–34]. On the other hand, the donor acceptor charge transfer site in this molecule is similar to that of reported molecule 4-dimethylamino benzaldehyde and JULCHO [46,47]. Rettig et al. [47] reported single emission band of JULCHO at ~400 nm in acetonitrile solvent. They did not find any large Stokes shifted band in case of JULCHO in polar solvents. Hence they proposed that charge transfer process in JULCHO is not feasible in the excited state may be due to restriction of donor torsion which is a pre-requisite for ICT emission according to TICT model.

However, it is also reported that tertiary amino donor group locked by ring to the aromatic centre in tetrahydroisoquinoline (THIQ) shows dual fluorescence where flipping at the nitrogen site of the flexible six member ring is responsible for this excited state CT process and is known as flipped intramolecular charge transfer process [48–50]. Interestingly, the parent molecule julolidine on the other hand shows low frequency large amplitude nitrogen inversion motion coupled with ring puckering motion in the gas phase [51]. Keeping in mind about the ICT in THIQ, low-frequency large-amplitude motion in julolidine and presence of stronger acceptor group in THBQC suitable for ICT process and also proton donor acceptor sites responsible for ESIPT we are interested to study the possible ICT and ESIPT process in THBQC. We have studied the photophysical properties of THBQC by steady state and time resolved spectroscopy in the condensed phase. In addition, we have performed structural and ground state PES calculations at HF/6-31G** as well as DFT/B3LYP/6-31G** level. We have evaluated the excited state potential energy surfaces of THBQC at different levels-one is at CIS/6-31G** and another is TDDFT/6-31G** level to correlate the experimental findings with theoretical calculations to support ESIPT process in THBQC molecule.

2. Experimental

2.1. Materials

The sample THBQC (Chart 1) purchased from Aldrich was used as supplied. Spectroscopic grade solvents such as cyclohexane (CYC), *n*-heptane (HEP), tetrahydrofuran (THF), methanol (MeOH), ethanol (EtOH), and acetonitrile (ACN) from Spectrochem were used for preparing different solutions. Sulphuric acid (H_2SO_4), Sodium Hydroxide (NaOH) and triethylamine (TEA) from E Merck were used as supplied.

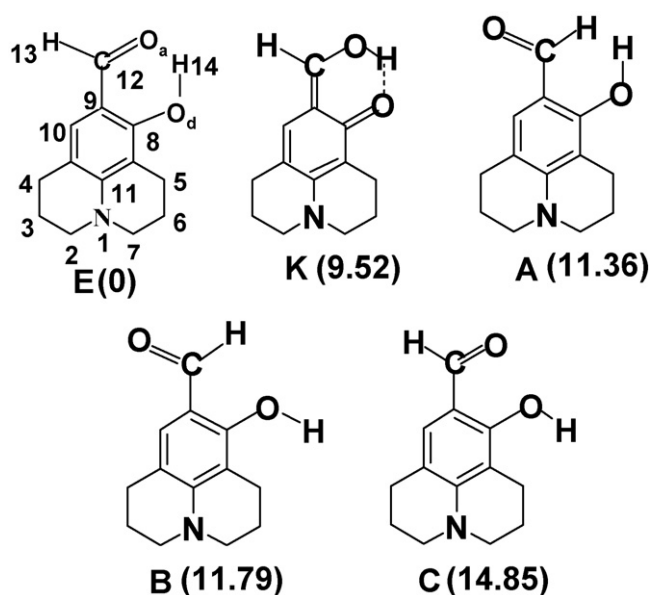


Chart 1. Different possible ground state low energy conformers of THBQC calculated by DFT(B3LYP/6-31G**) method. (Energies of the different conformers relative to the E-form in kcal/mole is given in parentheses).

Triple distilled water was used for the preparation of aqueous solutions.

2.2. Absorption and emission measurement

The absorption and emission spectra were measured by Hitachi UV–Vis U-3501 spectrophotometer and Perkin Elmer LS-50B spectrophotometer, respectively. In all measurements, the sample concentration was maintained within the range 10^{-4} – 10^{-5} mol/dm³ in order to avoid aggregation and re-absorption effects. Fluorescence life-time measurement has been done by time correlated single photon counting technique (TCSPC) at 54.7° magic angle with respect to polarization axis of the excitation beam. The TCSPC setup was from Edinburgh instruments, UK. In order to excite THBQC an excitation laser source of wavelength 375 nm (instrument response function, 73 ps) was used [52].

2.3. Theoretical calculations

The ground state structures and properties for all the possible low energy conformers of THBQC were computed using HF and DFT methods with 6-31G** basis set using Gaussian 03 software [53]. For the evaluation of the potential energy surfaces (PES) along the proton transfer coordinate, the ground state intramolecular proton transfer curves (GSIPT) were calculated using the energies of both the RHF/6-31G** and B3LYP/6-31G** fully optimized geometry at fixed O_d – H_{14} (Chart 1) distances over the range of 0.90–1.8 Å.

The excited state PESs were obtained by calculating the Franck–Condon transition energies for the HF/6-31G** as well as B3LYP/6-31G** ground state structures at the CIS and TDDFT level. The Franck–Condon curves for the proton transfer process were obtained by adding the CIS/6-31G** and TDDFT/6-31G** excitation energies to the corresponding GSIPT curves at HF and DFT levels, respectively. The strength of the IMHB (E_{IMHB}) was estimated from the difference between the energy of the fully optimized molecular structures of the non-hydrogen bonded form (with the -OH or -CHO group rotated 180° away from the H-bonded conformation) and the energy of the E-tautomer at B3LYP/6-31G** level.

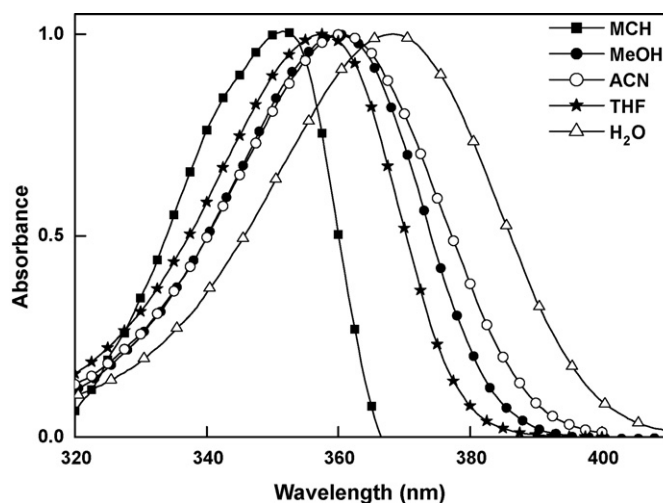


Fig. 1. Absorption spectra of THBQC in different solvents at room temperature.

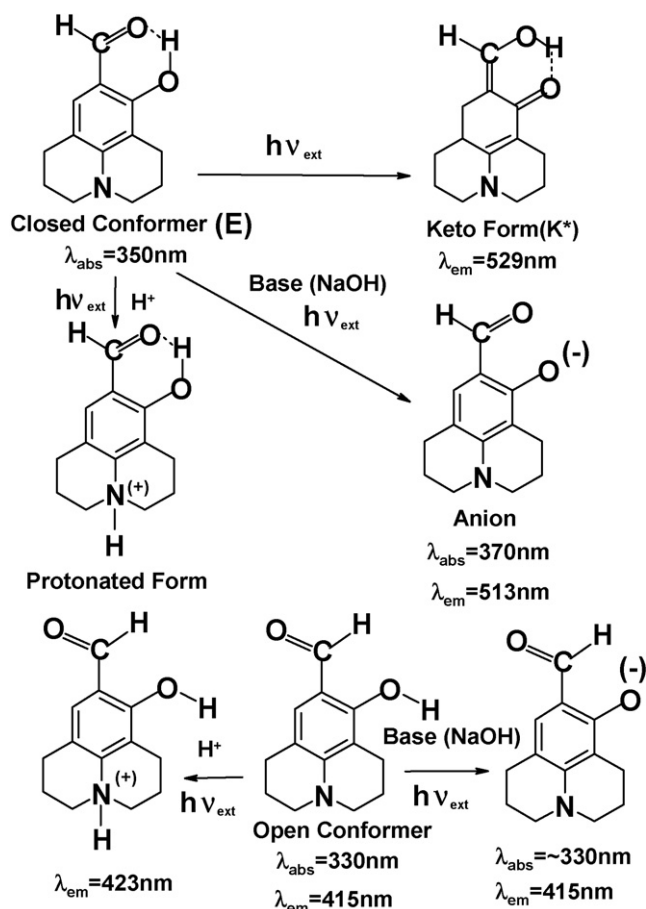
3. Results and discussion

3.1. Absorption spectra

The room temperature absorption spectra of THBQC have been measured in different organic solvents such as non-polar, polar aprotic and polar protic solvents and are shown in Fig. 1. All spectral data have been presented in Table 1. As seen in the absorption spectra, the molecule THBQC exhibits a single broad absorption band with a weak shoulder at the blue side and the absorption maximum is found to be slightly red shifted with increasing solvent polarity. The absorption maxima is observed at ~350 nm in non-polar and at ~361 nm in polar solvents (Fig. 1). The weak blue sided shoulder is seen at ~330 nm. The spectral pattern is almost similar to that of OHBA molecule. It is to point out that the target molecule THBQC has two basic subunit units—one is the salicaldehyde unit where possible intramolecular hydrogen bonding between O_d and H_{14} atoms is responsible for ESIPT reaction (Chart 1) and the other unit comprises of aldehydic group and a locked tertiary amino group attached to the aromatic ring may show CT reaction as was seen in THIQ molecule. It is reported that the basic unit OHBA and JULCO molecule absorbs at 325 nm and 350 nm, respectively, for their π – π^* type of transition [28–34,47]. Due to the presence of tertiary amino, hydroxyl and aldehyde sub-

Table 1
Observed spectral bands obtained from absorption and emission spectra of THBQC at room temperature

Solvents	Absorption band (nm)	Emission band (nm)		Quantum yield of low energy band (ϕ_K)
MCH	350	–	523	3.82×10^{-4}
CYC	350	–	523	4.19×10^{-4}
HEPT	350	–	523	3.75×10^{-4}
THF	358	415	525	6.28×10^{-4}
CCl ₄	355	416	525	5.26×10^{-4}
ACN	361	415	532	7.92×10^{-4}
EtOH	360	415	529	7.68×10^{-4}
MeOH	361	415	529	8.06×10^{-4}
MeOH + ACID	361	423	529	–
MeOH + BASE	370	415	513	–
H ₂ O	370	415	529	6.29×10^{-5}



Scheme 1. Different ground and excited species of THBQC in various media.

stitution in the chromophore ring of THBQC the $\pi-\pi^*$ type of transition shifts to the red compared to benzene. Analogous to OHBA, the single broad absorption band with a weak blue sided shoulder in THBQC may indicate the existence of two conformers in the ground state as was found in OHBA. As per the assignment in OHBA, the strong absorption band at 350 nm may arise from the most stable lowest energy hydrogen bonded closed conformer of the molecule (Scheme 1). Other weak band may be the high-energy solvated open conformer having less population in the ground state and hence the absorption band intensity is low. Detailed quantum chemical calculations of the structural isomers are discussed in the theoretical section. As was observed for reported donor acceptor charge transfer species the slight red shift of the absorption maxima with increasing solvent polarity may be due to little charge separation between the nitrogen and carbon of aldehyde group because of difference of electronegativity in THBQC.

3.2. Effect of acid and base

Due to the presence of acidic OH group (phenolic OH) and lone pair of nitrogen the spectral characteristics of THBQC can be influenced by acid and base. It is seen that the absorption spectra of THBQC in methanol do not change in presence of electron donor weak base triethylamine (TEA). On the other hand, when we add strong base such as NaOH in the methanolic solution

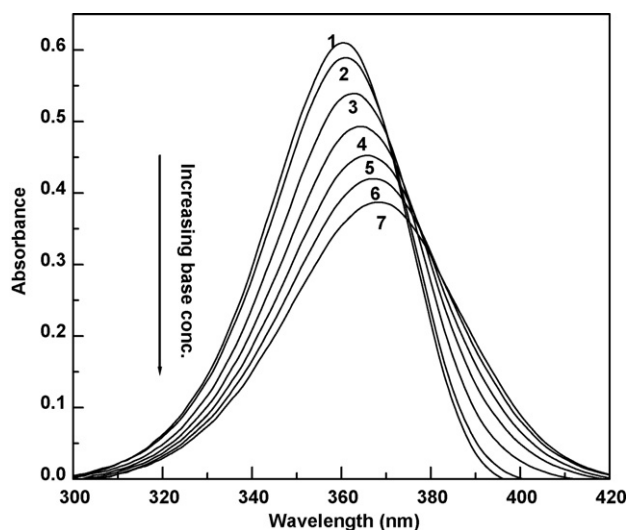


Fig. 2. Effect of addition of base NaOH on the absorption spectra of THBQC in methanolic solution at room temperature: (1) without base and (2–7) with increasing $[\text{OH}^-]$ concentration (0.29 mM, 0.58 mM, 0.87 mM, 1.16 mM, 1.45 mM and 1.74 mM).

of THBQC the absorption maxima is red shifted to ~ 370 nm from ~ 361 nm with concomitant decrease in absorbance value (Fig. 2). Very similar observation was observed in case of OHBA molecule [33,34]. The position of absorption maxima of OHBA in EtOH solution shifted on addition of base and the new red shifted band was assigned to the anion of OHBA in the ground state [33,34]. Thus, the new band at ~ 370 nm in the absorption spectra is assigned to the anion of the closed conformer of THBQC (Scheme 1) generated by abstraction of proton and breaking of intramolecular hydrogen bond. In the ground state, the strongly hydrogen bonded closed conformer does not allow the weak base TEA to form the anion. However, strong base NaOH can easily rupture intramolecular hydrogen bond and forms anion in polar solvents. But the formation of anion in non-polar media does not take place on addition of TEA or NaOH, probably due to the presence of strong intramolecular hydrogen bonding in these non-interfering solvents. The less populated open conformer present in the ground state may also form anion in presence of base, but the absorption peak for its anion is weak and hence it is suppressed by the strong anion band for the closed conformer.

Gradual addition of dilute H_2SO_4 to the methanolic solution of THBQC does not affect the absorption spectra and the position of the band maximum is found to be unchanged. The probable sites of attack by the H^+ ion are the O-atoms and the N-atom. The availability of the lone pair on the N-atom makes it more susceptible to be attacked by the H^+ ion compared to that of O-atoms for both the conformers. Hence, protonation at N-atom of the tertiary amino group is more likely to take place resulting in formation of protonated species which may have the absorption maxima in close proximity with the bare molecule and hence the position of the band maxima remains unchanged. Whereas, in case of molecules exhibiting charge transfer process, addition of acid results in shifting of the absorption maxima to the blue [4,6–9]. This is due to unavailability of lone pair of nitrogen

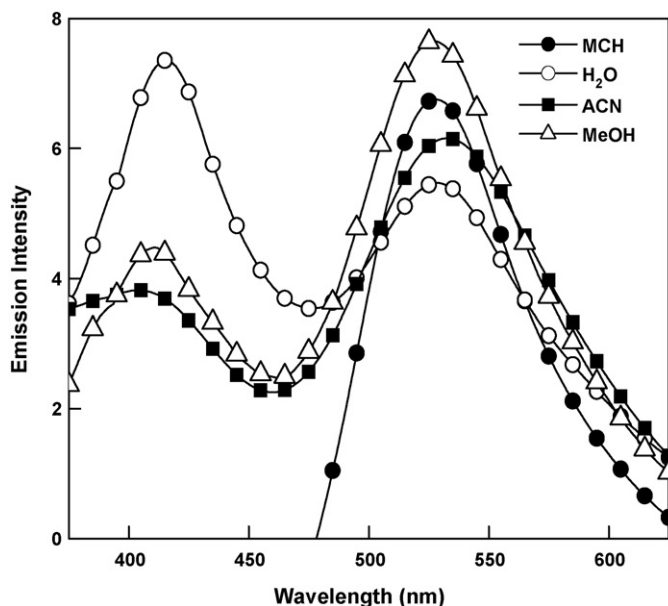


Fig. 3. Emission spectra ($\lambda_{\text{ext}} = 350 \text{ nm}$) of THBQC in different solvents having different polarity at room temperature.

upon protonation and resonance delocalization is absent in the protonated species. This possibility is absent in case of THBQC as the N-atom is locked and protonation of its lone pair hardly results in any electronic reorganization.

3.3. Fluorescence emission and excitation spectra

Figs. 3 and 4 depict the emission and excitation spectra, respectively, of THBQC in different solvents. It is seen that THBQC exhibits a large Stokes shifted fluorescence in all non-polar hydrocarbon solvents and dual fluorescence bands in polar solvents. Unlike the absorption spectra, the emission spectra of THBQC have negligible solvent dependency and the fluo-

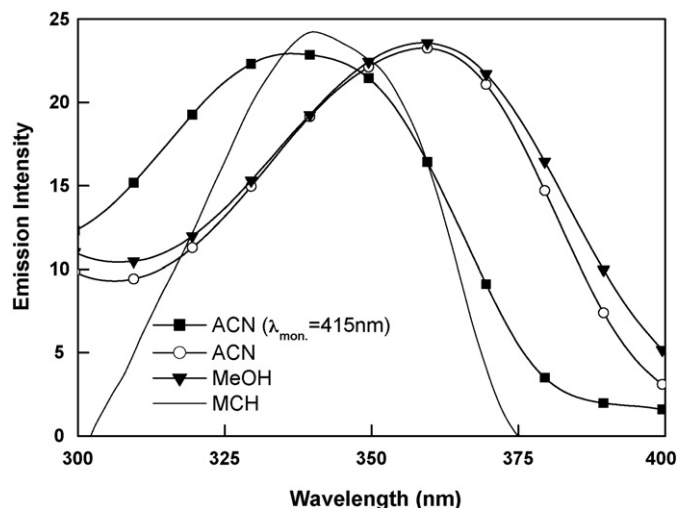


Fig. 4. Fluorescence excitation spectra of THBQC in non-polar and polar solvents at room temperature: (—) in MCH ($\lambda_{\text{emi}} = 523 \text{ nm}$), (—○—) in ACN ($\lambda_{\text{emi}} = 529 \text{ nm}$), (—■—) in ACN ($\lambda_{\text{emi}} = 415 \text{ nm}$) and (—▼—) in MeOH ($\lambda_{\text{emi}} = 529 \text{ nm}$).

rescence maximum of the low energy emission band is found to undergo a slight bathochromic shift with increasing solvent polarity (Fig. 3). This observation indicates that the species formed in the excited state is of neutral character and hence can be the keto tautomer as was observed in case of OHBA molecule [33,34]. All the spectral data are presented in Table 1 and the spectral observations are summed up below.

In non-polar hydrocarbon solvents, for example in cyclohexane, THBQC exhibits a broad emission band at $\sim 523 \text{ nm}$ ($\lambda_{\text{ext}} = 350 \text{ nm}$). It is interesting to note that in non-polar solvents there is only one emission band at $\sim 523 \text{ nm}$ which is quite similar to that of the parent molecule OHBA [28–34]. It is to point out that the molecule JULCO shows only local emission at $\sim 400 \text{ nm}$. Interestingly, 2-hydroxy-4-dimethylamino benzoic acid methyl ester, a molecule having both the donor acceptor CT and proton transfer sites, shows simultaneously CT and ESIPT at 435 nm [54]. Therefore, the emission band of THBQC at $\sim 523 \text{ nm}$ could not be the emission from any CT state as CT band should not be observed in non-polar solvents. Nagaoka et al. [29] observed only a single broad emission band of OHBA in this region (525 nm) corresponding to the emission from the keto form generated by ESIPT process in non-polar solvents. However, the molecule methyl salicylate (MS) exhibits dual emission from locally excited state and proton transfer species. Experimentally it is found that in case of MS the barrier height for this keto-enol isomerization in the excited state lies in the range of $\sim 3.7\text{--}4.7 \text{ kcal/mole}$ in methylcyclohexane solvent whereas that obtained for OHBA is $\sim 1.7 \text{ kcal/mole}$ and hence OHBA shows only PT emission due to low barrier height [29]. In case of polar solvents (aprotic as well as protic) two emission bands are observed for THBQC, a higher energy emission band at $\sim 415 \text{ nm}$ and another relatively more intense lower energy emission band in the range of $\sim 525\text{--}530 \text{ nm}$. Similar dual fluorescence was observed by Nagaoka et al. [29] for OHBA in polar protic solvents with emission maxima at $\sim 420 \text{ nm}$ and $\sim 520 \text{ nm}$ and the emission bands are assigned to emission from the open solvated conformer and the keto tautomer, respectively. Fig. 4 depicts the excitation spectra monitored at 525 nm emission band which matches reasonably well with the absorption spectra in all solvents. But in case of the higher energy emission band, i.e., 415 nm band, the excitation spectra does not match with the absorption spectra (Fig. 4). This spectral mismatch indicates that the emission stems from a species that exists as a minority in the ground state or may be from in the higher excited state of THBQC. Interestingly the position of the excitation band maxima for 415 nm emission band is same as that of the weak high-energy absorption band. Interestingly similar high-energy band was observed for OHBA in polar protic solvents by Nagaoka et al. [29] and they assigned this to the emission from the open solvated conformer of the molecule. In analogy to this observation, the lower wavelength emission band ($\sim 415 \text{ nm}$) of THBQC can be assigned to the solvated open form which has minor existence in the ground state. This assignment of the 415 nm emission band of THBQC is supported after a thorough analysis of the variation of intensity of emission band with varying pH and temperature of the medium (later sections).

3.4. Fluorescence quantum yields

The fluorescence quantum yield for the low energy emission band of THBQC has been measured by the secondary standard method using the equation given below and the results are presented in Table 1. The molecule β -naphthol is used as secondary standard ($\Phi = 0.23$ in methylcyclohexane) [2].

$$\Phi_f = \Phi_f^\circ \frac{n_0^2 A^\circ \int I_f(\lambda_f) d\lambda_f}{n^2 A \int I_f(\lambda_f) d\lambda_f}$$

where n_0 and n are the refractive indices of the solvents, A° and A are the absorbances, Φ_f° and Φ_f are the quantum yields, and the integrals denote the area of the fluorescence bands for the standard and the sample, respectively. It is found that the fluorescence quantum yield of the low energy emission band is low and is similar to that of OHBA [33]. In water, quantum yield of lower energy band (keto form) of THBQC is very low ($\Phi_f = 6.29 \times 10^{-5}$) and may be due to the fact that hydrogen bonding can favor energy wash out through some non-radiative channels.

3.5. Fluorescence life time

The presence of different emitting species in the excited state can be determined by fluorescence lifetime measurement. The fluorescence decay curves of THBQC have been monitored in non-polar, polar aprotic and polar protic solvents at room temperature (Fig. 5). Intensity decay curves were fitted as a sum of exponential terms: $F(t) = \sum_i \alpha_i \exp(-t/\tau_i)$ where α_i is a pre-exponential factor representing the fractional contribution to the time resolved decay of the component with a life time τ_i . The fluorescence lifetime of 523 nm emission band is fitted with biexponential decay and for each solvent the decay curve shows a short component with maximum contribution and a long

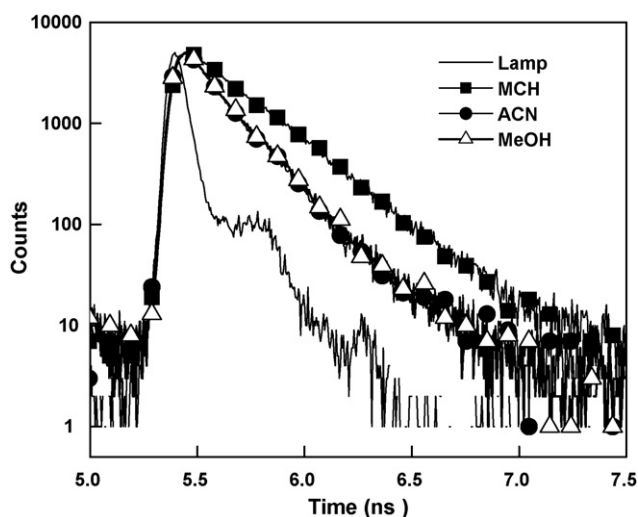


Fig. 5. Typical decay profiles of THBQC in MCH ($\lambda_{\text{monitored}} = 523$ nm), ACN and MeOH ($\lambda_{\text{monitored}} = 529$ nm) at 298 K. The curves represent the best fit of the experimental points to a single exponential decay. Excitation wavelength = 375 nm; the lamp profile is given.

component with minor contribution. It is found that the short lifetime of major contributing and long lifetime minor contributing term are 213 ps (93.25%) and 477 ps (6.75%), respectively, in *n*-heptane ($\alpha_1 = 0.079$, $\alpha_2 = 0.003$, $\chi^2 = 1.127$). The lifetime of the same major and minor contributing terms are 133 ps (97.35%) and 510 ps (2.65), respectively, in acetone solvent ($\alpha_1 = 0.093$, $\alpha_2 = 0.001$, $\chi^2 = 1.077$) and 135 ps (98.06%) and 1406 ps (1.94%), respectively, in methanol solvent ($\alpha_1 = 0.094$, $\alpha_2 = 0.000$, $\chi^2 = 1.331$). It is to point out that the fluorescence decay for the proton transfer form of OHBA is in the order of picoseconds time scale [28,29] and that of CT band of *N,N*-dimethylaminobenzaldehyde and THIQ is in the order of nanoseconds time scale [46,48]. The ultrafast fluorescence decay for the red sided emission band in THBQC is similar to that of OHBA molecule. The emission at 523 nm arises from the K^* form where the short fluorescence lifetime in all type of solvents indicates that prior to the emission from the K^* state the excited state proton transfer process must be very fast. The comparatively low fluorescence lifetime in protic solvent (MeOH) indicates that hydrogen bonding interaction insists non-radiative channel and that is also reflected in the low quantum yield data.

3.6. Effect of acid and base

It is found that both the increase and decrease of pH has shown remarkable effect on the emission spectral properties of THBQC. Gradual addition of aqueous solution of NaOH in MeOH solution of THBQC results in a blue shift of the emission maxima of lower energy band upto ~ 513 nm from 529 nm and the hypsochromic shift is about 16 nm (Fig. 6a). Excitation spectrum of ~ 513 nm emission band in basic medium correlates well with the absorption spectrum of THBQC in MeOH in presence of NaOH. Thus, the strong emission band at ~ 513 nm is assigned to the anion of the closed conformer, which is formed due to abstraction of proton by the addition of base as shown in Scheme 1. The large Stokes shifted fluorescence of the anion is attributed to its capability of resonance stabilization by extensive delocalization of the negative charge over the benzene π -electrons. The weak intense band at the higher energy side may correspond to the anion of the open solvated form. Base has no effect on the emission spectra of THBQC in non-polar solvents and as is observed in the absorption spectra. This is due to the presence of strong intramolecular H-bonding in THBQC in non-polar solvents, which cannot be ruptured even by strong base.

On addition of dilute H_2SO_4 in MeOH solution of THBQC, the high-energy emission band (~ 415 nm) increases its intensity and low energy emission band (529 nm) decreases its intensity (Fig. 6b). In addition, the higher energy band at ~ 415 nm is red shifted upto ~ 423 nm. Usually, for donor acceptor CT system, the red shifted CT emission band reduces its intensity largely on addition of acid due to protonation at nitrogen lone pair and unavailability of lone pair for CT process. Therefore, the red shifted band in THBQC is no doubt the emission from proton transfer state instead of CT state. The molecule THBQC exists as two conformers in the ground state with minor abundance of the open solvated form and major abundance of closed form.

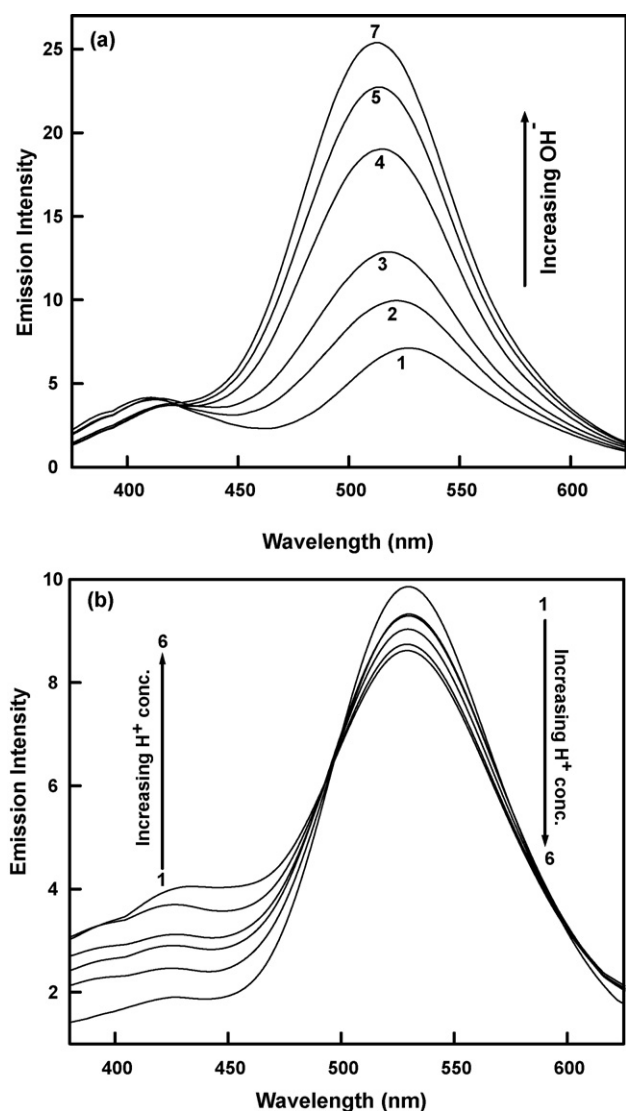


Fig. 6. (a) Effect of addition of base NaOH on the emission spectra of THBQC in methanolic solution at room temperature: (1) without base and (2–7) with increasing $[\text{OH}^-]$ concentration (0.29, 0.58, 0.87, 1.16, 1.45 and 1.74 mM) (b) Effect of acid on emission spectra ($\lambda_{\text{ext}} = 523$ nm) on addition of acid in methanolic solution of THBQC at room temperature (298 K), (1) without acid and (2–6) with increasing $[\text{H}^+]$ concentration.

Hence, both the protonated closed and open solvated form can show their local emission. This new 423 nm band is probably due to emission from the protonated species of the open conformer of THBQC molecule (Scheme 1). The decrease in intensity of the lower energy emission band at ~ 529 nm is probably due to decrease in population of the normal molecule on addition of acid to the medium and hence formation of keto form becomes less feasible in acidic media. However, even at high concentration of acid the band at ~ 529 nm persists. First of all the protonated closed conformer may have its local emission at the same place of the keto form. Secondly deprotonation of the protonated closed conformer may occur in the excited state resulting in the formation of the E^* form which ultimately facilitates the formation of K^* form. Hence, the deprotonation process of the closed conformer in the excited state can give PT emission.

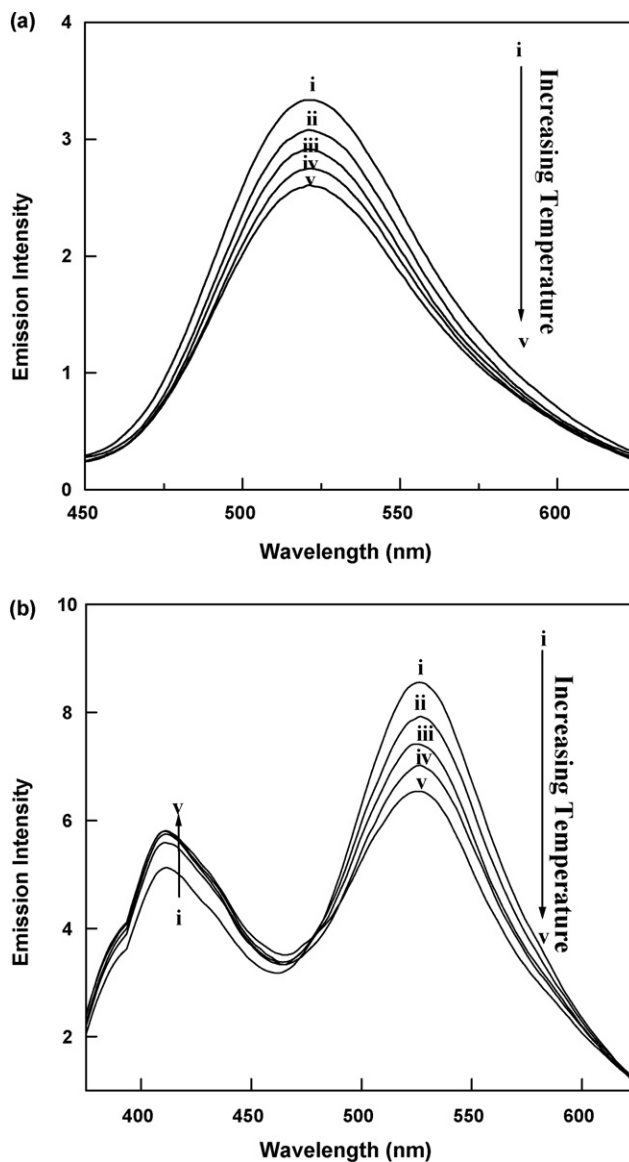


Fig. 7. (a) Temperature effect on the emission spectra ($\lambda_{\text{ext}} = 523$ nm) in methyl cyclohexane solution above room temperature (298 K), (b) Temperature effect on emission spectra ($\lambda_{\text{ext}} = 523$ nm) in methanolic solution above room temperature (298 K). (i) 298 K, (ii) 308 K, (iii) 318 K, (iv) 328 K, and (v) 338 K.

3.7. Effect of temperature

Variation of temperature has pronounced effect on the emission spectra of THBQC in both the polar and non-polar solvents. The effect of temperature further reinforced our assignment of different emitting species. In case of non-polar solvent such as cyclohexane the lower energy emission band at ~ 523 nm shows a decrease in intensity with increasing temperature. However, the position of the emission maxima remains unchanged throughout (Fig. 7a). In case of polar protic solvents, with increase of temperature, the lower energy emission band (~ 529 nm) shows a decrease in intensity and a concomitant increase in intensity of the higher energy band at ~ 415 nm (Fig. 7b). Here a point is to note that in polar solvents, the above mentioned observation is made only above room temperature. Below room tempera-

Table 2

Relevant calculated structural parameters for the ground and excited state optimized geometry of THBQC at HF and DFT levels

Parameters	HF/6-31G** level (E-form)		HF/6-31G** level (K-form)		DFT/B3LYP/6-31G** level [#]	
	G.S.	E.S.	G.S.	E.S.	E-form	K-form
O _d -H	0.953	0.970	1.600	1.600	1.003	1.600
C ₈ -O _d	1.331	1.311	1.239	1.240	1.344	1.273
C ₈ -C ₉	1.403	1.484	1.460	1.472	1.422	1.467
C ₉ -C ₁₂	1.451	1.428	1.358	1.379	1.437	1.378
C ₁₂ -O _a	1.206	1.235	1.294	1.315	1.243	1.312
N ₁ -C ₁₁	1.362	1.384	1.372	1.392	1.384	1.382
O _d ...O _a	2.684	2.578	2.491	2.495	2.596	2.539
∠C ₈ -O _d -H ₁₄ (°)	109.75	109.28	119.87	119.16	106.14	101.46
∠C ₁₁ -N ₁ -C ₂ -C ₃ (°)	41.93	45.25	36.96	47.30	36.65	33.91
∠C ₁₁ -N ₁ -C ₇ -C ₆ (°)	-44.98	-44.78	-48.30	-42.60	-40.84	-39.63
Dipole moment (D)	5.67	7.17	5.61	5.26	5.680	5.442

G.S. and E.S. are ground and excited states, respectively.

[#] For ground state.

ture with increasing temperature, both the emission bands show a decrease in intensity. Similar observation was made in polar aprotic solvents too. So from the above observations it is clear that in non-polar solvents the intensity of the 523 nm emission band decreases with increase of temperature due to the increase possibility of non-radiative channels at higher temperatures. But in case of polar solvents, with increase of temperature the emission intensity of the 529 nm band decreases with concomitant increase in intensity of lower energy emission band at 415 nm possibly due to formation of the open conformer from the closed conformer with the breaking of intramolecular hydrogen bond by heating. Since the calculated strength of the hydrogen bond being ~ 15 kcal/mole, agitation upon heating may result in rupture of this bond [5].

3.8. Quantum chemical calculation

The conformational landscapes of THBQC molecule are explored in the electronic ground state by DFT as well as HF method and the relevant structural parameters for the E- and K-form are presented in Table 2. Different low energy computed structures with respect to the position of hydroxy and aldehyde groups for the ground state are shown in Chart 1. Out of all possible structures it is seen that the intramolecularly hydrogen bonded closed form (E-form) is more stable than any other form of THBQC. Intramolecular hydrogen bond also stabilizes the K-form compared to any of the open conformers (Chart 1). As seen in Fig. 8a and b, DFT calculations yields energies (E in kcal/mole) for different electronic states with the variation of torsional angle (ι) at the hydroxyl and aldehyde sites separately. The strength of IMHB (E_{IMHB}) for the E-form has been determined to be 14.85 kcal/mol by rotating the phenolic OH group out of the H-bonded configuration (Fig. 8a) and computing the energy difference between closed (E-form) and open form (C-form). Similar calculation has been carried out by rotating the aldehyde group out of the H-bonded configuration and the strength of IMHB (E_{IMHB}) for E-form is determined to be 11.36 kcal/mole (Fig. 8b). For all the conformers, the N-atom lies in the plane of the aromatic π -ring system and hence the lone pair is just parallel to that of the aro-

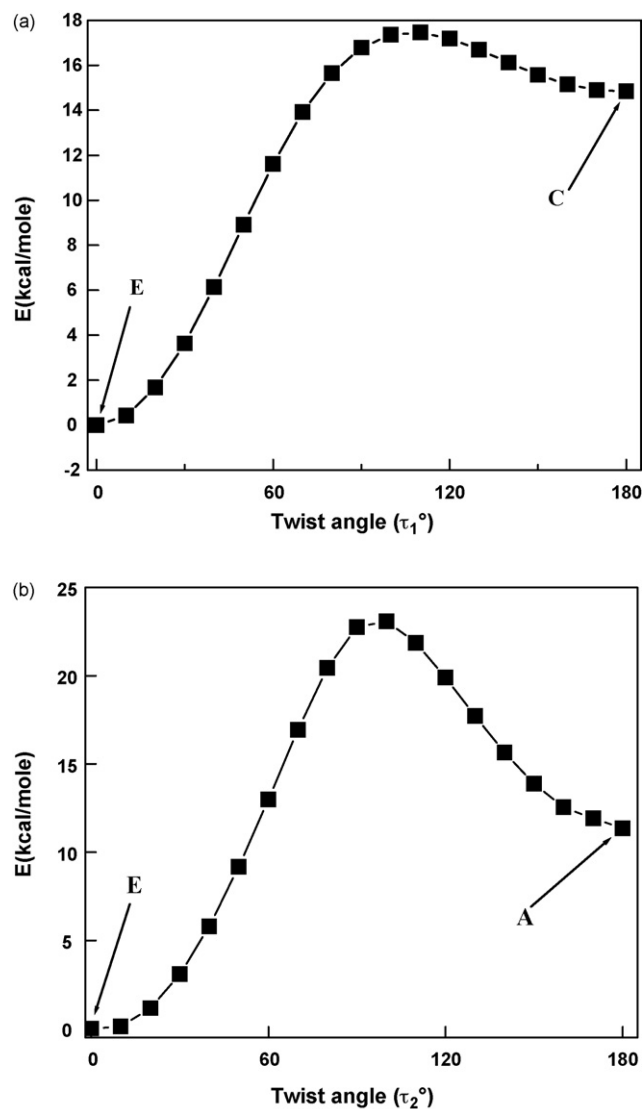


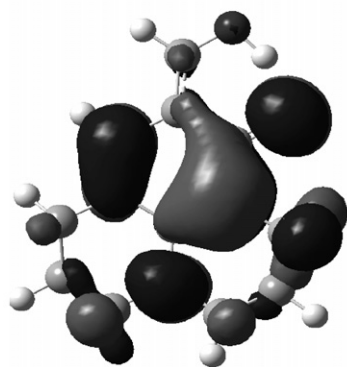
Fig. 8. (a) Variation of energy during the transformation from E to C form of THBQC by twisting angle (ι_1) at DFT(B3LYP/6-31G**) level. (b) Variation of energy during the transformation from E to A form of THBQC by twisting angle (ι_2) at DFT(B3LYP/6-31G**) level.

matic π -electron system enabling extensive delocalization of the charge.

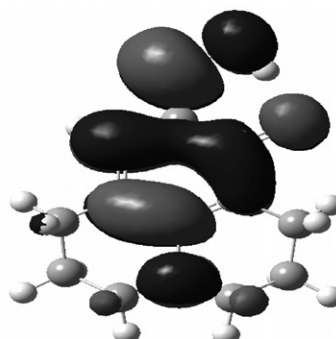
The optimized parameters for the ground state of the E- and K-forms at HF and DFT levels and the excited state at CIS level using 6-31G** basis set are given in Table 2. For both the HF and DFT levels the ground state structural parameters for the E- and K-forms are similar in nature. It is seen from the calculated data at HF/6-31G** level (Table 2) that the O_d -H₁₄ bond length for the E-form (Chart 1) increases from 0.953 Å to 0.970 Å from ground state (G.S.) to the excited state (E.S.). Similarly, the $O_d \cdots H_{14} \cdots O_a$ bond angle of the E-form increases from 143.39° to 149.32° and $O_d \cdots O_a$ bond distance decreases from 2.684 Å to 2.578 Å from ground to the excited state. Interestingly, the $O_d \cdots H_{14} \cdots O_a$ bond angle (149.25°) and $O_d \cdots O_a$ bond distance (2.495 Å) for the K-form (HF/6-31G**) is found to be closer to that of the excited state parameters of the E*-form. Therefore, this structural change of bond length and bond angle for going from ground to the excited state of E-form indicates the possibility of proton transfer in the excited state. Examination of the computed negative charge distribution from Mulliken Scheme at HF/6-31G** level shows an increase in negative

charge distribution on O-atom of -CHO group from ground to the excited state (-0.603 in G.S. to -0.640 in E.S.). Simultaneously negative charge distribution decreases on O-atom of the -OH group (-0.678 in G.S. to -0.672 in E.S.). This also supports the possibility of proton translocation from -OH group to -CHO group of THBQC on excitation. It is probable that on excitation THBQC attains a delocalized excited state, which then relaxes to the proton transfer configuration with the transfer of proton from -OH group to -CHO group. A geometrical rearrangement is required during the transformation from E-form to K-form for both the ground and excited state. As seen in the Table 2, $O_d \cdots O_a$ bond length decreases more in the ground (-0.106 Å) compared to the excited state (-0.004 Å) for the transformation E- to K-form at Hartree-Fock level. And similar type of change is observed in case of $\angle O_d \cdots H_{14} \cdots O_a$ angle. Here the $\angle O_d \cdots H_{14} \cdots O_a$ angle increases more in the ground state (+5.93°) compared to that of the excited state (+1.14°) for the transformation E-form to K-form. The change in dipole moment from ground to the excited state for both the E- and K-form is not so significant (Table 2). Therefore, it is expected that the position of the emission maxima of the K* form should remain nearly independent of solvent polarity and this tallies

K Form

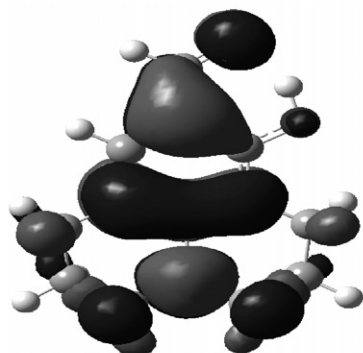


HOMO

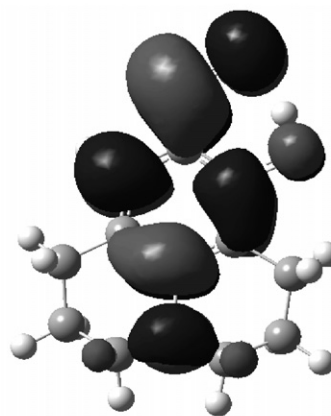


LUMO

E Form



HOMO



LUMO

Fig. 9. HOMO-LUMO of the E- and K-forms of THBQC calculated using B3LYP/6-31G** level.

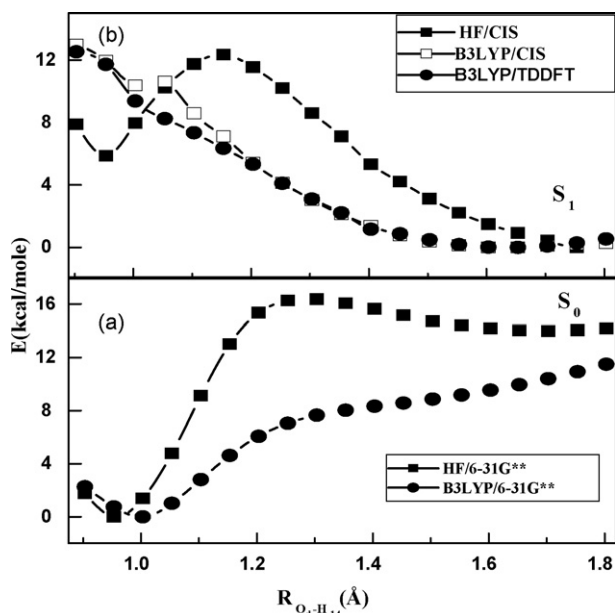


Fig. 10. Energy variation along the $R_{O_d-H_{14}}$ distance from the enol to the keto tautomer of THBQC. Calculated for (a) the ground state (S_0) at the HF and B3LYP levels using 6-31G** basis set and (b) the first excited state (S_1) at the CIS and TDDFT levels using the same basis set as used in ground state.

with the experimental observation (Table 1). As seen in Table 2, the calculated parameters are similar at both HF and DFT levels for the E- and K-form.

As shown in Fig. 9, the HOMO-LUMO pictures can provide a clear representation of the electronic distribution for the E- and K-forms. For both the E- and K-forms ($R_{O_d-H_{14}} = 1.6 \text{ \AA}$) the HOMO and LUMO orbitals are of π and π^* character, respectively. The HOMO also has a larger electronic projection over O_a in the E-form with small electronic projection over the O -atom (i.e. O_d) of the OH group. But in the LUMO of E-form the electronic projection over the O_a of IMHB ring is greatly enhanced indicating greater possibility of transfer of the proton to the O_a -atom in the excited state. The HOMO of K-form shows higher electronic projection at O_d -atom. For the LUMO of K-form, the electronic projection increases over O_d compared to LUMO of E-form as well as the HOMO of K-form. Thus, the orbital pictures clearly favour proton transfer in the excited state but not in the ground state. Furthermore, it can be seen that the electron density remains more or less localized on the IMHB of the LUMO orbital of the K-form with antibonding character between O_a and O_d , C_8 and O_d , C_{12} and O_a and between C_{12} and C_9 . This situation hinders back ES IPT process [26].

Fig. 10 shows the variation of potential energy of THBQC along a selected reaction coordinate computed at different levels of theory. To construct PES we have optimized the structure at each point keeping the O_d-H_{14} bond length fixed value ranging between 0.9 Å and 1.8 Å. It can be seen in Fig. 10a that the energy of the S_0 state increases with the increase of O_d-H_{14} bond length by B3LYP/6-31G** method. In B3LYP/6-31G** method, there is only one minima at the enol form (E) in the ground state (S_0). But for the HF/6-31G** method, the ground state has an asymmetric double well character (Fig. 10a). So at HF/6-31G** method there are two minima—one for the enol form (E) and another for the keto form (K) in the ground state (S_0). The E-form is the global minima and K-form is local minima. The energy difference between the E and K form is about 16 kcal/mole. From Fig. 10b, it can be seen that the S_1 state also shows an asymmetric double well type potential along the reaction coordinate (O_d-H_{14} bond length), with two minima obtained by HF/CIS method. On the other hand, DFT/TDDFT and DFT/CIS methods shows a single minimum at K^* form. In all the methods for the S_1 state, the K^* -form is more stable than the E^* -form and the proton transfer process is nearly a barrierless process in case of DFT/TDDFT and DFT/CIS methods. On the other hand, in case of HF/CIS method there is a small barrier (barrier height ~ 6.5 kcal/mole) for the transformation from E^* - to K^* -form. Experimentally it is seen that in case of non-polar solvents there is no dual fluorescence, only K^* emission is observed. So DFT/CIS and DFT/TDDFT method is more supportive with the experimental results than the HF/CIS method. No such double well character is observed in the S_2 state (Figure not given). Thus, this calculation accounts for a facile barrierless proton transfer reaction in the S_1 state. Table 3 shows the theoretical and experimental values for the vertical excitation energy and oscillator strength computed at DFT and HF levels using 6-31G** basis set. As is evident from the data, the theoretical values of absorption maxima (315 nm) in vacuo at TDDFT/B3LYP/6-31G** level is quite in agreement with the experimental value of 350 nm in methylcyclohexane. The theoretical emission wavelength (401 nm) at the same level can be correlated with the experimentally emission band in MCH solution (523 nm). The above values obtained at CIS/6-31G** level does not correlate so well with the experimental data. We have computed the vertical excitation energy (Table 3) for the open conformer (B-form) at TDDFT/B3LYP/6-31G** method (Chart 1). The computed $S_0 \rightarrow S_1$ transition energy for the open conformer is found to be 3.72 eV (~ 333 nm). It is about 18 nm red shifted from the closed conformer. But the oscillator strength for the above transition is very low compare to the closed conformer and this

Table 3

Comparison of vertical excitation energy of THBQC at TDDFT/6-31G** and CIS/6-31G** level (in parantheses) with experimentally obtained value in MCH solvent

Transition type	Vertical energy (eV)	Wavelength (nm)	Oscillator strength*	Experimental value in MCH (nm)
$S_0 \rightarrow S_1$ (E \rightarrow E*) Closed form	3.9297 (4.8620)	315.51 (255.10)	0.0197 (0.3863)	350.00
$S_1 \rightarrow S_0$ ($K^* \rightarrow$ K) Closed form	3.0907 (3.7378)	401.25 (331.71)	0.0315 (0.1516)	523.00
$S_0 \rightarrow S_1$ (E \rightarrow E*) Open form	3.721	333.20	0.0002	–

* Oscillator strength values obtained at TDDFT/6-31G** and CIS/6-31G** level (in parentheses).

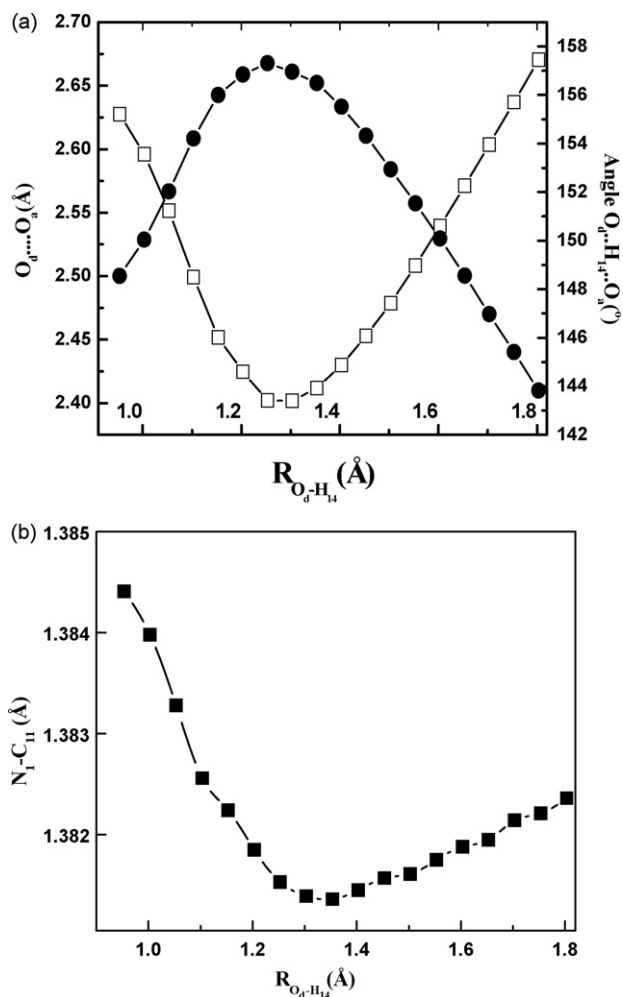


Fig. 11. (a) Variation of $O_d \cdots O_a$ bond distance (—□—) and $O_d \cdots H_{14} \cdots O_a$ bond angle (—●—) with $R_{O_d-H_{14}}$ distance using B3LYP/6-31G**, (b) Variation of N_1-C_{11} bond as a function of O_d-H_{14} length at B3LYP/6-31G** level.

correlates well with the weak blue sided band in the absorption spectra.

It is found for several studied systems that the PESs for the ES IPT process are multidimensional in nature and in our case the structural change also predicts similar indication (Table 2) [10–12]. During the process of proton transfer from O_d to O_a , it is expected that almost all the coordinates undergo some changes [4–6]. As seen in Table 2, the main structural changes are the $O_d \cdots O_a$ and N_1-C_{11} bonds, and $O_d \cdots H_{14} \cdots O_a$ angle. Since the vital coordinate is the O_d-H_{14} distance, the variation of PE is observed along this coordinate only (Fig. 10) and theoretical results favour a barrierless excited state proton transfer process. As seen in Fig. 11a, it is found that the midway through the proton transfer process, the $O_d \cdots O_a$ distance contracts to a minimum and the angle $O_d \cdots H_{14} \cdots O_a$ increases to a maximum before relaxing to the K-form. A crossover point between E- and K-form is found at around OH distance of 1.3 Å. These calculations were performed at HF level too and the trends remained the same. Interestingly, the N_1-C_{11} bond length decreases with increase of O_d-H_{14} distances and passing through a minimum at

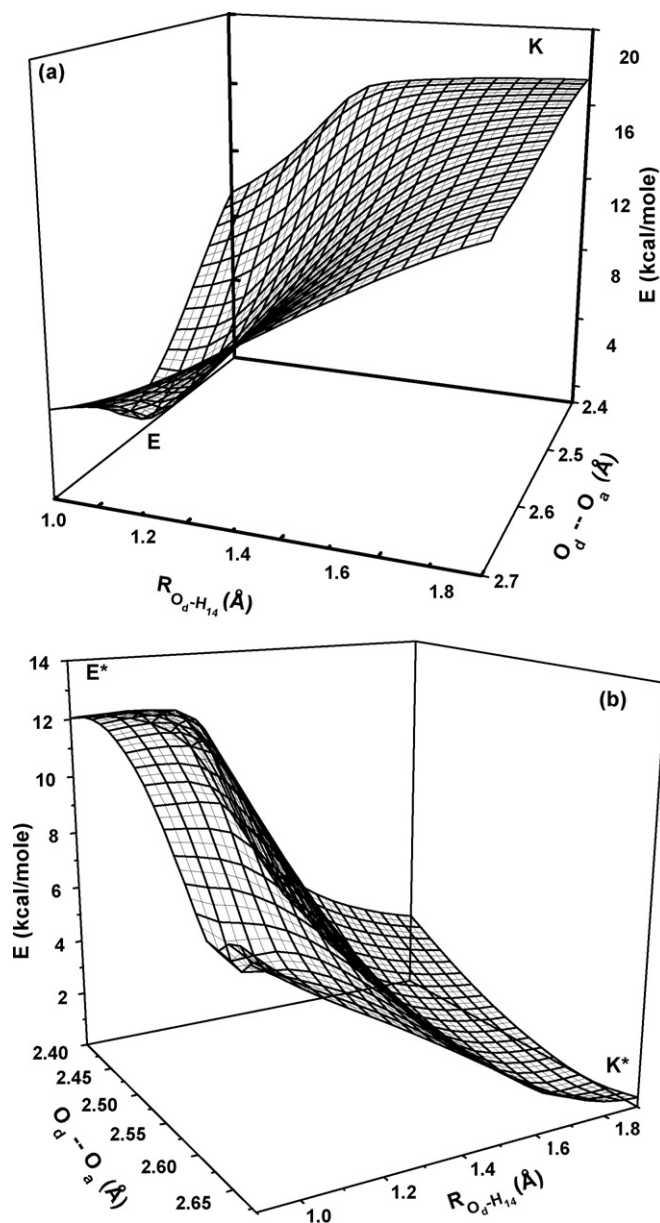


Fig. 12. 3D plot of the variation of PES for the (a) ground state using DFT and (b) excited state using TDDFT level as a function of O_d-H_{14} and $O_d \cdots O_a$ distances.

OH distance of 1.3 Å (Fig. 11b). From Fig. 11b it is seen that the N_1-C_{11} bond length decreases sharply with increase in O_d-H_{14} bond length. This sharp decrement is upto $O_d-H_{14} = 1.35$ Å and after that the N_1-C_{11} bond length increases to a small extent with the increase of O_d-H_{14} bond length. Thus, Fig. 11a and b indicate that no matter which coordinate is followed during the proton transfer process, in all cases, the crossover point from E- to K-form remains at ~ 1.3 Å. Fig. 12a and b show the 3D plots of PESs with simultaneous variation of O_d-H_{14} and $O_d \cdots O_a$ co-ordinates for the ground and excited states, respectively. The energy in the 3D plot is given in Kcal/mole with respect to the minimum of each state. In the S_0 state, a single well corresponds to the E-form whereas in the S_1 state, the single well corresponds to the K*-form. These results predict that the E-form of

the molecule upon excitation can only give K^* emission. The calculated PES also shows that the generated K^* state relaxes to the unstable ground keto form through a red shifted emission and finally goes to the stable E-form.

4. Conclusion

From the experimental and theoretical data it may be concluded that the molecule THBQC exists as intramolecular hydrogen bonded closed conformer and a open solvated form in the ground state. The closed conformer exhibits ESIPT process in all solvents leading to observed red shifted emission from the keto tautomer. The less solvent polarity dependence of the Stokes shifted band predicts only ESIPT reaction but not the ICT reaction in this molecule. Both the conformers can form anion by strong base and protonated species in presence of acid and each of the anions and cations have their own characteristic absorption and emission properties. Quantum chemical calculations at HF and DFT levels predict that the closed conformer is the most stable in the ground state but in the first excited state the keto form is more stable. The one dimensional or multidimensional nature of the theoretical PESs along the proton transfer coordinates favour a barrierless keto-enol isomerisation in the excited state leading to a red shifted emission band from the keto tautomer.

Acknowledgement

NG acknowledges DST, India (Project No.SR/S1/PC-1/2003) for financial support. The authors are thankful to Dr. Samir K. Pal and Ajay K. Shaw of S.N.Bose Centre for Basic Science, Kolkata, for allowing them to use fluorescence lifetime measuring instrument. SM and RBS are also grateful to CSIR, New Delhi for Senior Research fellowship.

References

- [1] A.Z.Z. Weller, *Electrochem.* 60 (1956) 1144.
- [2] S.J. Formosinho, L.G. Arnaut, *J. Photochem. Photobiol. A* 75 (1993) 21.
- [3] Z.R. Grabowski, K. Rotkiewicz, A. Siemiarczuk, D.J. Cowley, W. Bauermann, *Nouv. J. Chim.* 3 (1979) 443.
- [4] Z.R. Grabowski, K. Rotkiewicz, W. Rettig, *Chem. Rev.* 103 (2003) 3899.
- [5] A. Sytnik, M. Kasha, *Proc. Natl. Acad. Sci.* 91 (1994) 8627.
- [6] A. Chakraborty, S. Kar, D.N. Nath, N. Guchhait, *J. Phys. Chem. A* 110 (2006) 12089.
- [7] A. Chakraborty, S. Kar, N. Guchhait, *J. Photochem. Photobiol. A* 181 (2006) 246.
- [8] A. Chakraborty, S. Kar, N. Guchhait, *Chem. Phys.* 320 (2006) 75.
- [9] A. Chakraborty, S. Kar, N. Guchhait, *Chem. Phys.* 324 (2006) 733.
- [10] S. Mahanta, R.B. Singh, S. Kar, N. Guchhait, *Chem. Phys.* 324 (2006) 742.
- [11] R.B. Singh, S. Mahanta, S. Kar, N. Guchhait, *Chem. Phys.* 331 (2007) 189.
- [12] R.B. Singh, S. Mahanta, S. Kar, N. Guchhait, *Chem. Phys.* 331 (2007) 373.
- [13] H. Mishra, S. Maheshwary, H.B. Tripathi, N. Sathyamurthy, *J. Phys. Chem. A* 109 (2005) 2746.
- [14] P.T. Chou, M.L. Martinez, W.C. Copper, C.P. Chang, *Appl. Spectrosc* 48 (1994) 604.
- [15] D.G. Ma, F.S. Liang, L.X. Wang, S.T. Lee, L.S. Hung, *Chem. Phys. Lett.* 358 (2002) 24.
- [16] P.T. Chou, M.L. Martinez, S.L. Studer, *Appl. Spectrosc* 45 (1991) 918.
- [17] J. Keck, H.E.A. Kramer, H. Port, T. Hirsch, P. Fischer, G. Rytz, *Phys. Chem. A* 100 (1996) 144468.
- [18] J. Catalan, J.C. Delvalle, F. Fabero, N.A. Garcia, *Photochem. Photobiol.* 61 (1995) 118.
- [19] A. Sytnick, M. Kasha, *Proc. Natl. Acad. Sci. USA* 91 (1994) 8627.
- [20] Y. Kubo, S. Maeda, S. Tokita, M. Kudo, *Nature* 382 (1996) 522.
- [21] L.B. Feringa (Ed.), *Molecule Switches*, Wiley-VCH Weinheim, Germany, 2001.
- [22] *Photochromism, Memories and Switches*, *Chem. Rev.* 100 (2000) (Special issue).
- [23] A.J.A. Aquino, H. Lischka, C. Hattig, *J. Phys. Chem. A* 109 (2005) 3201.
- [24] A.L. Sobolewski, W. Domcke, *J. Phys. Chem. A* 108 (2004) 10917.
- [25] A.L. Sobolewski, W. Domcke, *Phys. Chem. Chem. Phys.* 1 (1999) 3065.
- [26] J. Catalan, J. Valle, J. Palomar, C. Diaz, J.L.G. De Paz, *J. Phys. Chem. A* 103 (1999) 10921.
- [27] J. Catalan, J. Palomar, J.L.G. De Paz, *J. Phys. Chem. A* 101 (1997) 7914.
- [28] S. Nagaoka, N. Hirota, M. Sumitani, K. Yashihara, E. Lipczynska-Kochany, H. Iwamura, *J. Am. Chem. Soc.* 106 (1984) 6913.
- [29] S. Nagaoka, N. Hirota, M. Sumitani, K. Yashihara, *J. Am. Chem. Soc.* 105 (1983) 4220.
- [30] T. Nishiyama, S. Yamauchi, N. Horota, Y. Fujiwara, M. Itoh, *J. Am. Chem. Soc.* 108 (1986) 3880.
- [31] S. Nagaoka, U. Nagashima, N. Ohta, N.M. Fujita, T. Takemura, *J. Phys. Chem.* 92 (1988) 166.
- [32] T. Nishiyama, S. Yamauchi, N. Hirota, M. Baba, I. Hanazaki, *J. Phys. Chem.* 90 (1986) 5730.
- [33] J. Catalan, F. Toribio, A.U. Acuna, *J. Phys. Chem.* 86 (1982) 303.
- [34] U. Nagashima, S. Nagaoka, S. Katsumate, *J. Phys. Chem.* 95 (1991) 3532.
- [35] A. Douhal, F. Lahmani, A. Zewail, *Chem. Phys.* 207 (1996) 477.
- [36] S. Lochbrunner, A.J. Wurzer, E. Riedle, *J. Chem. Phys.* 112 (2000) 10699.
- [37] S. Lochbrunner, T. Schultz, M. Schmitt, J.P. Shaffer, M.Z. Zgierski, A. Stolow, *J. Chem. Phys.* 114 (2001) 2519.
- [38] S. Lochbrunner, K. Stock, V. De Waele, E. Riedle, in: A. Douhal, J. Santamaria (Eds.), *Femtochemistry and Femtobiology: Ultrafast Dynamics in Molecular Science*, World Scientific, River Edge, NJ, 2002, p. 202.
- [39] A.L. Sobolewski, W. Domcke, in: D. Heidrich (Ed.), *The Reaction Path in Chemistry: Current Approaches and Perspectives*, Kluwer Academic Publishers, Dordrecht, The Netherlands, 1995, p. 257.
- [40] A.L. Sobolewski, W. Domcke, *Phys. Chem. Chem. Phys.* 8 (2006) 3410.
- [41] P.F. Barbara, L.E. Brus, R.P.M. Rentzepis, *J. Am. Chem. Soc.* 102 (1980) 5631.
- [42] K.A. Zachariasse, M. Grobys, Th. von der Haar, A. Hebecker, Yu.V. Il'ichev, O. Morawski, I. Rückert, W. Kuhnle, *J. Photochem. Photobiol. A* 105 (1997) 373.
- [43] W. Schuddeboom, S.A. Jonker, J.M. Warman, U. Leinhos, W. Kuhnle, K.A. Zachariasse, *J. Phys. Chem.* 96 (1992) 10809.
- [44] A.D. Walsh, *J. Chem. Soc.* (1953) 2288.
- [45] T. Fournier, S. Pommeret, J.-C. Mialocq, A. Deflandre, R. Rozot, *Chem. Phys. Lett.* 325 (2000) 171.
- [46] S. Dahne, W. Freyer, K. Tenchner, J. Dobkowski, Z.R. Grabowski, *J. Lumin.* 22 (1980) 37.
- [47] W. Rettig, B. Zietz, *Chem. Phys. Lett.* 317 (2000) 187.
- [48] P.K. Bera, A. Chakraborty, M. Chowdhury, *Chem. Phys. Lett.* 277 (1997) 52.
- [49] N. Guchhait, S. Banerjee, A. Chakraborty, D.N. Nath, G.P. Naresh, M. Chowdhury, *J. Chem. Phys.* 120 (2004) 9514.
- [50] A. Chakraborty, N. Guchhait, S. Banerjee, D.N. Nath, G.P. Naresh, M. Chowdhury, *J. Chem. Phys.* 115 (2001) 5184.
- [51] S. Bandyopadhyay, N. Guchhait, A. Chakraborty, D.N. Nath, M. Chowdhury, *Chem. Phys. Lett.* 346 (2001) 387.
- [52] A.K. Shaw, S.K. Pal, *J. Photochem. Photobiol. B* 86 (2007) 199.
- [53] M.J. Frisch et al., *Gaussian 03*, Revision B.03, Gaussian Inc., Pittsburgh PA, 2003.
- [54] D. Gormin, M. Kasha, *Chem. Phys. Lett.* 153 (1988) 574.